Austin Journal of Nanomedicine & Nanotechnology

Open Access

Austin Publishing Group

Special Article - Future Perspectives in the Surface Chemistry of Medical Devices

Synthesis and Simulation of Nano-Composite Metamaterial for Broadband Negative Refractive Index in Visible Spectral Regime

Keshavarz M[1], Rostami A[2]*, Dolatyari M[2]*, Rostami GH[2] and Khosravi S[2]

[1]Photonics and Nanocrystal Research Lab (PNRL), Faculty of Electrical and Computer Engineering, University of Tabriz, Tabriz, Iran

[2]SP- EPT Labs, ASEPE Company, Industrial Park of Advanced Technologies, Tabriz, Iran

***Corresponding author:** Rostami A, SP- EPT Labs, ASEPE Company, Industrial Park of Advanced Technologies, Tabriz, Iran

Dolatyari M, SP- EPT Labs, ASEPE Company, Industrial Park of Advanced Technologies, Tabriz, Iran

Received: March 18, 2021; **Accepted:** April 12, 2021; **Published:** April 19, 2021

Abstract

In this paper, a nano-metamaterial with the structure of Ag-SiO_2-PbTe is proposed that has a random arrangement in the host medium of expanded polystyrene (foam) for the realization of a broadband negative refractive index at the visible spectrum. The negative refractive index for the purposed meta-material was obtained from the plasmonic resonance in the core and outer layer for both electric and magnetic components of light. Here, we use different radii for the outer layer of nanoparticles to create the broadband negative permeability. In this way, the doped semiconductor nanoparticles are included in the host medium to create the broadband negative permittivity. The overlap between the spectrum of the negative permittivity and permeability introduces the broadband negative refractive index at the visible band. The novel introduced structure creates the broadband negative refractive index and it is simple and practical for fabrication. For the realization of the proposed material, synthesis and characterization of the designed nanocomposite structure are investigated. To this end, the absorption and the transmission coefficients of the synthesized material are measured and compared with theoretical results. The obtained results indicate that the numerical simulations using Mie theory have good agreement with the experimental results.

Keywords: Metamaterials; Broadband negative refractive index; Plasmonic; Nano-composite; Nano-particle

Introduction

Metamaterials have opened a new area in optical engineering. The researches on metamaterials (composite materials) over the last years have been unveiled. These composite materials have electromagnetic properties that transcend them from naturally occurring media. One of the characteristics of the metamaterials is their tunability in managing the refractive index in spanning positive, zero, and negative values. Based on these properties, metamaterials have enabled remarkable advances in invisibility cloaking [1-4], perfect optical absorption [5], bandpass filter [6], perfect lens [7], nano-antenna [8], and seismic metamaterials [9]. For creating the negative refractive index, negative permittivity and negative permeability in desired wavelength range are needed. Noble metals (such as silver, gold, and copper) have negative permittivity under plasma frequency; however, in high frequencies, natural materials have permeability about one, and negative permeability is limited to the hundreds of Gigahertz (GHz). For solving this problem we should create magnetic resonance by using artificial structures (metamaterials).

Formerly metamaterials were conceived as periodic arrays of sub-wavelength split-ring resonators. Operational wavelengths for these structures are in microwave frequencies [10,11]. Some metamaterials with fishnet, layered and strip structures are in high frequencies [12-18], and some structures that have 40nm-50nm bandwidth are in optical frequencies [16,17]. In these composites, constituent resonators exhibit electric and magnetic resonances based on their material compositions. By overlapping these negative resonances effective permittivity and permeability, and the negative effective refractive index can be achieved. Some of these structures have a negative refractive index in the broadband frequencies [12] that has a negative refractive index in broadband terahertz frequencies; however, these structures need to have high-resolution lithography for high frequencies. So, all of the mentioned structures have limitations for fabrication in the optical regime.

Plasmonic devices have been developed rapidly in recent years [19]. Interaction between metamaterials and plasmonics can exhibit some extraordinary phenomena and cause premier applications [20]. Notable specific plasmonic structures have been created by Metalo-dielectric layered structures in spherical nano-particles. These structures have been widely studied due to promising applications in nano-electronics. Therefore, core-shell structures have been explored as alternative metamaterials [21,22]. Recently a simple three-layered core-shell structure consisting of metal-core and dielectric shells have been found to exhibit some special optical properties [23]. This structure shows an electric and magnetic resonance at optical frequencies. However, this structure has only 40nm bandwidth in visible regime with a fill factor of 0.5, and one of the limitations for the fabrication of this structure is applying a vacuum environment [23]. So despite the significant progress in composite metamaterials and plasmonic devices, the fabrication of spectrally broadband negative-index metamaterials at the optical frequencies is one of the important challenges.

Citation: Keshavarz M, Rostami A, Dolatyari M, Rostami GH and Khosravi S. Synthesis and Simulation of Nano-Composite Metamaterial for Broadband Negative Refractive Index in Visible Spectral Regime. Austin J Nanomed Nanotechnol. 2021; 9(1): 1063.

All of the above structures have been discussed theoretically in the literature and there is no practical result for this purpose; because finding a suitable substrate to insert nano-particles in it is very difficult. Here we introduce new flexible material as a substrate with a refractive index near the vacuum and synthesis of a suitable nano-composite for this purpose.

In this way, we synthesized a three-dimensional isotropic nano-composite metamaterial consisting of spherical nano-particles that were included in a host medium (foam) (in 552-655 nm). We could broaden the bandwidth of the negative refractive index by about 103 nm in optical frequencies that have not been reported till now in optical frequencies with random and isotropic distribution with a fill factor of 0.45 [23,24]. The nanocomposite is prepared by Ag, SiO_2, and PbTe layers as a core, Middle (ML), and Outer Layers (OL) respectively and this nanocomposite is inserted in a polymer as the host medium which the polymer is expanded polystyrene named as foam. This structure has an electric and magnetic resonance at optical frequencies. Negative permittivity can be exhibited by the Ag core and negative permeability can be provided by the OL shell. To create negative permittivity in broadband frequencies, we use doped semiconductors. Superposition effect for nanocomposites with different diameters investigated to create the negative permeability in broadband frequencies. So overlap between negative permittivity and negative permeability leads to a negative refractive index in the optical regime. The designed flexible metamaterial is a novel composite material with a refractive index near the vacuum that has not been reported till now.

The electric and magnetic scattering coefficient of this structure is calculated using the Mie theory. Effective parameters (ε_{eff} and μ_{eff}) of random distribution for the nano-particles are obtained by Lorena-Lorenz theory. So, here, we introduce (theoretically and experimentally) a structure with the broadband negative refractive index over the visible spectrum regime with 3-D, isotropic, homogenous, and flexible nano-composite metamaterial.

Theory and Calculation of Effective Parameters

When metamaterials go to the optical regime, the involved metal begins to play a crucial role to determine the performance of metamaterials. Shen et al. have reported the different metals on the electromagnetic responses of metamaterials in optical regime [25]. Comparison of the performance of metamaterials made by different metals (i.e., gold, copper, silver) shows that silver is the best choice as the metal part of optical metamaterials to achieve a negative refractive index in optical regime (because silver has low intrinsic loss). In this paper, the main goal is to design a nano-composite metamaterial to achieve broadband negative refractive index in optical frequencies. To fulfill this propose we use the spherical core-shell nano-particles, inside the host medium of foam. To analyze this structure, we are going to apply Mie's theory. The extinction efficiency (Q_{ext}) can be expressed as [16]:

$$Q_{sca} = \frac{2}{y^2}\sum_{l=0}^{\infty}(2l+1)\left(|a_n|^2+|b_n|^2\right) \qquad (1)$$

where y=kR, k is wavenumber and R is the radius of the nano-particles. a_n and b_n are electric and magnetic scattering coefficients respectively.

Effective permittivity (ε_{eff}) and permeability (μ_{eff}) of a host medium with electric permittivity (ε_h) and magnetic permeability (μ_h) are calculated by using the Clausius-Mossotti equation:

$$\begin{cases} \dfrac{\varepsilon_{eff}-\varepsilon_h}{\varepsilon_{eff}+2\varepsilon_h} = f\dfrac{\alpha_E}{4\pi R^3} \\ \dfrac{\mu_{eff}-\mu_h}{\mu_{eff}+2\mu_h} = f\dfrac{\alpha_M}{4\pi R^3} \end{cases} \qquad (2)$$

where the electric and magnetic polarizabilities, (α_E and α_M respectively), are directly proportional to the scattering coefficients a_1 and b_1 by factor $i(k^3/6\pi)^{-1}$.

Simulation

In this paper, the permittivity of the metallic core is given by the Drude model as well as permittivity for ML and OL are constant. By analyzing the mutual influence of a metallic core with dielectric shells this question may be raised that how magnetic resonance is created in this structure. For the answer to this question, at first, we considered a metallic core without any shell in the host medium (foam). In this case, scattering coefficients of nano-particles, (a_n and b_n) for monolayer structure can be obtained from the given reference in part [26]. Figure 1 shows ε_{eff}, μ_{eff} and n_{eff} for Ag nano-particles with fill-factor 0.45 in the host medium of foam. The radius of the silver nano-particles is fixed at 40 nm and the refractive index of the foam is fixed in 1.017.

The metallic core has plasmon resonance at near-ultraviolet that arises from oscillations of conducted electrons; however, there is no magnetic resonance in the structure of Figure 1. To solve this problem, we can apply a dielectric shell around the core. Since the refractive index of the surrounding medium is smaller than the shell; the normal component of the field between the shell and surrounding medium causes a rotation and confinement of the electric field inside the shell. Since one important point in the characterization of metals is to avoid penetration of the field inside the metal; in a small metallic core no magnetic response is expected; consequently, the shell can manage the magnetic resonance. For two-layer core-shell metamaterial structure, expressions by the radius of a and b, a_n and b_n are obtained from the following equations [26].

$$a_n = \frac{\psi_n(y)\left[\psi_n'(m_2y)-A_n\chi_n'(m_2y)\right]-m_2\psi_n'(y)\left[\psi_n(m_2y)-A_n\chi_n(m_2y)\right]}{\xi_n(y)\left[\psi_n'(m_2y)-A_n\chi_n'(m_2y)\right]-m_2\xi_n'(y)\left[\psi_n(m_2y)-A_n\chi_n(m_2y)\right]} \qquad (3)$$

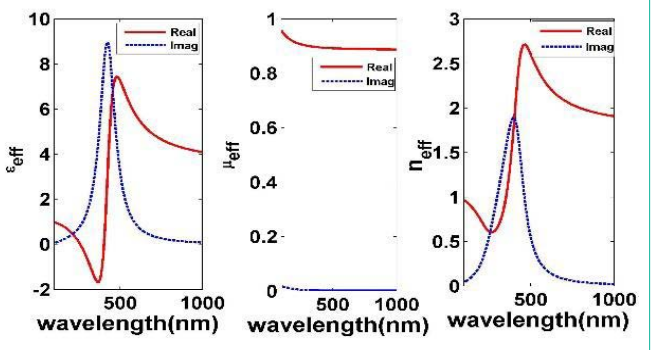

Figure 1: Effective permittivity, permeability, and refractive index for silver nanoparticles in the host medium of foam.

$$b_n = \frac{\psi_n(y)\left[\psi_n'(m_2y) - B_n\chi_n'(m_2y)\right] - m_2\psi_n'(y)\left[\psi_n(m_2y) - B_n\chi_n(m_2y)\right]}{\xi_n(y)\left[\psi_n'(m_2y) - B_n\chi_n'(m_2y)\right] - m_2\xi_n'(y)\left[\psi_n(m_2y) - B_n\chi_n(m_2y)\right]} \quad (4)$$

Where,

$$A_n = \frac{m_2\psi_n(m_2x)\psi_n'(m_1x) - m_1\psi_n'(m_2x)\psi_n(m_1x)}{m_2\chi_n(m_2x)\psi_n'(m_1x) - m_1\chi_n'(m_2x)\psi_n(m_1x)} \quad (5)$$

$$B_n = \frac{m_2\psi_n(m_1x)\psi_n'(m_2x) - m_1\psi_n(m_2x)\psi_n'(m_1x)}{m_2\chi_n'(m_2x)\psi_n(m_1x) - m_1\psi_n'(m_1x)\chi_n(m_2x)} \quad (6)$$

Here, $x=ka$, $y=kb$, and k is wave number. m_1 and m_2 are relative refractive indices of core and shell respectively. $X_n(x)=-xy_n(x)$, $\psi_n(x)=xj_n(x)$ and $\xi_n(x)=xh_n(1)(x)$ are Riccatti-Bessel functions and $h_n(1)(x)= j_n(x)+iy_n(x)$ is first class spherical Hankel function. Figure 2 shows an example for the electric and magnetic scattering of Ag-core and PbTe–shell in the host medium of foam. Here the radius of core and shell are fixed in 15nm and 75nm respectively. In this case, the refractive index of PbTe and foam are considered as constant numbers in optical frequencies (n_3=5.5 and n_4=1.017).

Figure 2 shows that the Ag core and PbTe shell have electric and magnetic dipole peaks at about 500nm and 800nm respectively. The electric resonance created by plasmon resonance in the core and magnetic resonance is due to electromagnetic resonance in the PbTe shell. However, in this case, electric and magnetic resonances have not any overlap on optical wavelength. Figure 3 shows a contour plot of electric and magnetic scattering spectra for Ag-PbTe nanoparticles as a function of R_{out} and R_{in}.

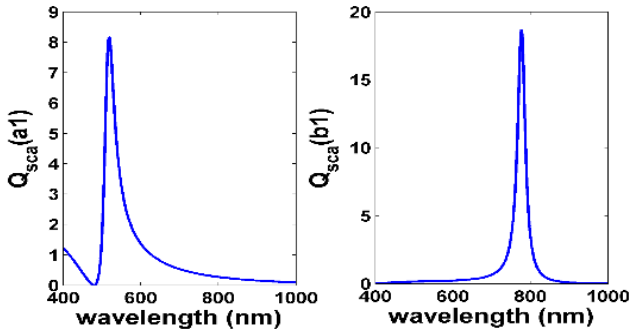

Figure 2: Electric and Magnetic resonances for two-layer structure by Ag core and PbTe shell in the host medium of foam.

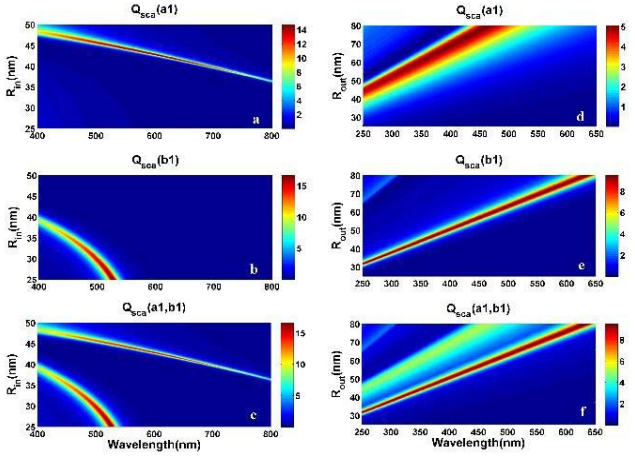

Figure 3: Contour plots of a) the Electric resonance, b) the Magnetic resonance, c) the Electric and Magnetic resonance for the Ag core and PbTe shell in the host medium of foam when the radius of core (R_{in}) is different and radius of the shell (R_{out}) is fixed in 51nm, d) the electric resonance, e) the magnetic resonance, f) the electric and magnetic resonance for the Ag core and PbTe shell in the host medium of foam when the radius of the shell (R_{out}) is different and radius of core(R_{in}) is fixed in 24nm.

Figure 3c and 3f shows that electric and magnetic resonances have not any overlap at optical frequencies for different radii of R_{in} and R_{out}; because their resonance frequencies are different. We should consider that increasing the radius of core and shell causes overlap between electric and magnetic resonance in the IR regime. So for solving this problem in optical frequencies such as the given reference in part [15], a middle layer with a lower refractive index should be used in the core-shell structure around the core. Figure 4 shows a three-layered core-shell structure. In this structure, we use Ag-SiO_2-PbTe as a core, middle and outer layer respectively. The refractive index of the middle layer can be considered as a constant number in optical frequencies (n_2=1.45). The outer layer acts as a cavity, and the middle layer around the core, decreases permittivity around the Ag core, and these phenomena increase the density of charge on the surface of the metal. The results show that the electrical resonance shifts to high frequencies. In this case, a_n and b_n, for three-layer core-shell structure, are obtained using the following expressions [27].

$$a_n = \frac{\psi_n(x_3)H_n^a(m_3x_3) - m_3D_n^{(1)}(x_3)}{\xi(x_3)H_n^a(m_3x_3) - m_3D_n^{(3)}(x_3)} \quad (7)$$

$$b_n = \frac{\psi_n(x_3)H_n^a(m_3x_3) - m_3D_n^{(1)}(x_3)}{\xi(x_3)H_n^a(m_3x_3) - m_3D_n^{(3)}(x_3)} \quad (8)$$

where $x_3=kr_3$ and m_3 is refractive index of outer layer; $D_n^{(1)}=\psi_n'(x)/\psi_n(x)$, $D_n^{(2)}=\chi_n'(x)/\chi_n(x)$, and $D_n^{(3)}=\xi_n'(x)/\xi_n(x)$ are the logarithmic derivatives of Ricatti-Bessel function.

Figure 5a and 5d, and Figure 5b and 5e show the scattering spectra of the Ag-SiO_2-PbTe nanoparticles as a function of radii of the middle layer (r_2) and the outer layer (r_3) for the electric and magnetic contributions respectively. Figure 5c and 5f shows the contour plot for the electric and magnetic scattering spectra of the Ag-SiO_2-PbTe nano-shells as a function of radii of the middle layer (r_2), and the outer layer (r_3) respectively. In Figure 5a-5e the radius of the core is fixed at 34nm, but, in Figure 5a-5c the radius of r_3 is fixed at 60nm, and in Figure 5d-5e the radius of r_2 is fixed at 39nm. In Figure 5c the electric and magnetic spectra have an overlap at about 600nm and 430nm. So for creating resonance in these wavelengths the radius of the middle layer should be considered as 39nm or 53nm. In Figure 5f the electric and magnetic spectra overlap at the wavelength of 600nm. In this case, the radius of the outer layer should be taken about 60-70 nm.

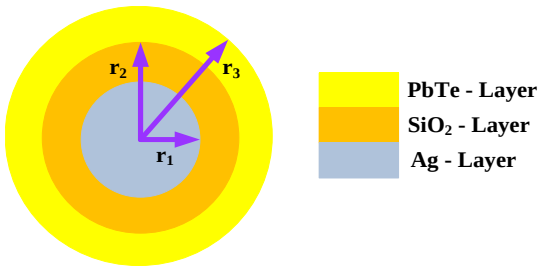

Figure 4: Schematic of the designed three-layer core-shell structure.

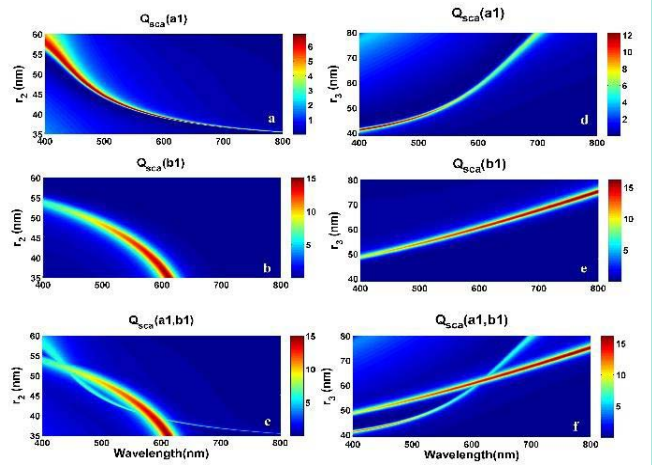

Figure 5: Contour plot of the, a) electric resonance, b) magnetic resonance, c) the electric and magnetic resonance together for the Ag-SiO_2-PbTe nano-shells as a function of the radius of the r_2, d) electric resonance, e) magnetic resonance, f) the electric and magnetic resonance together for the Ag-SiO_2-PbTe nano-shells as a function of the radius of the r_3.

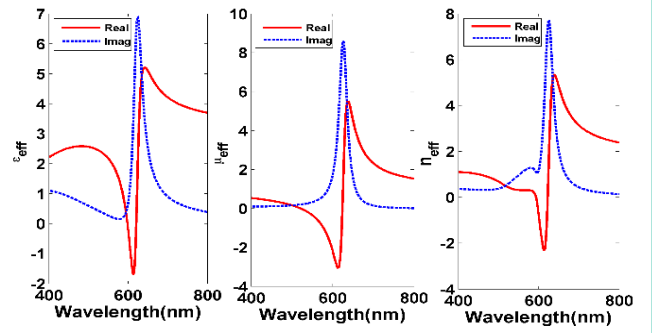

Figure 6: Real and imaginary parts of the effective permittivity, permeability, and refractive index of the Ag-SiO_2-PbTe for the random arrangement of nanoparticles as a function of wavelength with radii of 34nm, 39nm, and 62nm as core middle layer and outer layer respectively.

Result and Discussion

Figure 6 shows the real part (red curve) and imaginary part (blue curve) of effective permittivity, permeability, and refractive index of the Ag-SiO_2-PbTe nano-shells for the random arrangement of nano-particles as a function of wavelength. Here the radii of the core, middle layer, and outer layer are fixed on r_1=34nm, r_2=39nm, and r_3=62nm respectively. The electric and magnetic resonance peaks for this structure appear at about 600nm. The filling factor (f) of three-layer nanoparticles is considered to be 0.45. It is observed that the negative real part of the effective permittivity and permeability can be created at 608-630 nm and 547-655 nm respectively. So, an effective negative refractive index can be found at 600-640 nm.

One of the problems in Figure 6 is the narrowness of the band frequencies of the negative refractive index; because it has negative permittivity and permeability in narrowband frequencies. So, for solving this problem the band frequencies with negative permittivity and permeability should be broadened. Since, magnetic resonance is under the influence of radii of the outer layer, to broaden the band frequency with negative permeability we use different radii of the outer layers. In this case, the radii of the outer layer are considered to be r_3=60, 62, 63nm, and fill fraction of 0.12 [28]. Typically plasma frequencies of the metals are in ultra-violate spectra. By adding a shell with fixed permittivity, plasma frequencies can be shifted in optical spectra. However, in this case (Figure 6), the band frequencies with negative permittivity are so narrow. To solve this problem doped semiconductor nanoparticles are added to the foam as the host medium [18]. The required plasma frequency for metal nano-particles can be estimated as the following equation [29].

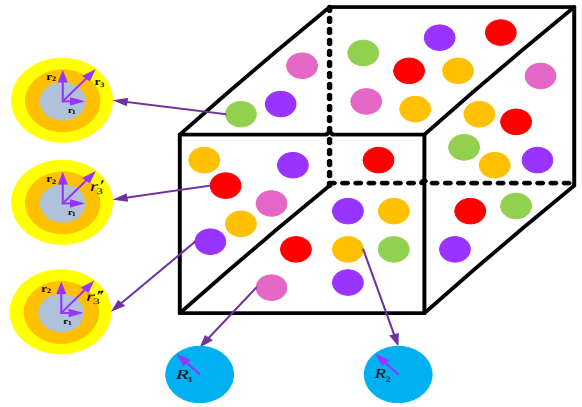

Figure 7: Schematic the Ag-SiO_2-PbTe nano-particles (red-violet and green particles) and semiconductor nano-particles (Brown and Pink particles) with random arrangement.

$$\omega_p = \omega_e^{res}\sqrt{\frac{3}{1-f}},\ \gamma = \omega_p/100 \qquad (9)$$

where ω_e^{res} is desired resonance frequency of ε_r^{eff} and f is the fill factor. So in this paper, we take two types of doped semiconductor nano-particles with the plasma frequency of 5.525×10^{15} Hz and 6×10^{15} Hz, with the radii of 20nm and 30nm respectively. The filling factor for each particle is 0.05. Figure 7 shows a schematic of the Ag-SiO_2-PbTe and semiconductor nano-particles with the random arrangement in the foam as host medium. Figure 8 shows the real part (red curve) and imaginary part (blue curve) of the effective permittivity, permeability, and refractive index for the structure showed in Figure 7. By applying the mentioned idea we can design broadband negative refractive index in optical frequencies.

Experimental Section

Processing the Expanded Polystyrene (EPS)

The 0.1g polystyrene was solved in 20cc benzene under ultra-sonication. The mixture was heated to 150°C under the protection of nitrogen and 20ml H_2O added to it at 150°C. When the mixture demand to dried, the mixture was cooled to room temperature and dried on glass [30].

Synthesis of the nano-particles (core-shell structures)

The Ag-SiO_2-PbTe core-shell structure as nano-particles in fabricated nano-composite metamaterials is synthesized by the following method in three steps.

Processing of Ag (core): In a typical process, for the synthesis of Ag (core), 0.166g Ag acetate and 10cc diethylene glycol were mixed under the protection of nitrogen at 220°C and a magnetic stirring rate of 400rpm. Then 1cc hydrazine monohydrate was injected in it for

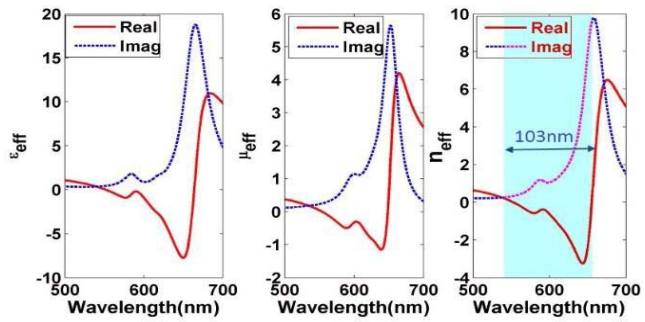

Figure 8: Real and imaginary parts of the effective permittivity, permeability and refractive index of the composite structure. The radius of core (r_1) and middle layer (r_2) are fixed in 34nm and 39nm, and the radii of the outer layer are fixed r_3=60nm, r'_3=62nm and r''_3=63nm with fill factor of 0.12 for each particle. The radius of the semiconductor nano-particles (R) is 20nm and 30nm with fill factor of 0.05 for each particle.

the reconstruction of Ag at 220°C for 30min. The obtained material is centrifuged with ethanol, acetone, and distilled water 3 times.

Processing of SiO_2 (middle layer): 0.02cc Tetraethyl orthosilicate and 2cc 2-propanol were mixed and added into the dispersed solution of synthesized silver nanoparticles. Then 1cc NH_4OH was immediately injected into the solution for the formation of SiO_2 at 220°C for 10min. The obtained material is centrifuged with ethanol, acetone, and distilled water 3 times.

Processing of PbTe (outer layer): 0.2g lead acetate was dispersed in 5cc 2-propanol and added into the synthesized Ag/SiO_2 (dispersed in 20cc diethylene glycol) at 220°C for 5min. Then 0.08g Te powder, 0.18g NaOH, 5cc 2-propanol, 1cc H_2O, and 5cc diethylene glycol were dissolved inside the laboratory pipe and when all of the Te powder was dissolved completely, 0.1g sodium borohydride was added and the color of the reaction changed to purple. Then this solution was injected into the solution at 220°C for 60min. In the end, 50cc H_2O was injected into it for stopping the reaction. The obtained material was centrifuged with ethanol, distilled water, and 2-propanol several times.

Processing the nano-composite

In a typical process, 0.059g polystyrene was solved in 5cc benzene. Then 0.048g core-shell material dispersed in 5cc H_2O and the obtained mixture was added to polystyrene solution. Then the mixture was heated at 220°C under the protection of nitrogen and a stirring rate of 400rpm. Finally, when the mixture demands to dry, it was cooled to room temperature and dried on glass.

Spectroscopic studies and Structural characterization

The refractive index of the EPS was studied *via* Ellipsometer (SE800). Surface morphology and distribution of the particles were studied *via* a TESCAN model MIR3 Scanning Electron Microscope (SEM). The crystal structure of nanoparticles was characterized by X-Ray Diffraction (XRD) on a Siemens D500 using Cu- radiation (λ=1.541 A°). UV-Vis Transmission and absorption spectra were recorded using SPEC ORD 250 spectrophotometer.

Experimental results

Figure 9a and 9b show the SEM and optical image of synthesized

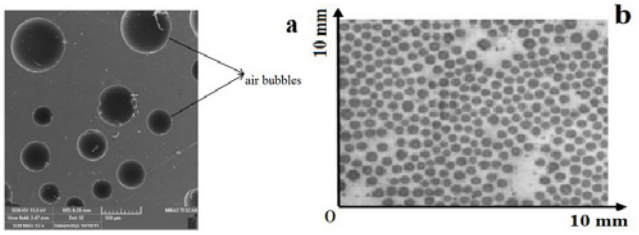

Figure 9: a) SEM and b) optical Images of the synthesized expanded polystyrene (foam).

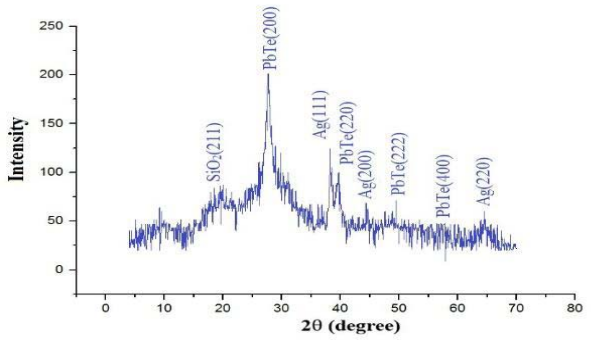

Figure 10: XRD pattern of the Ag-SiO_2-PbTe nanoparticles.

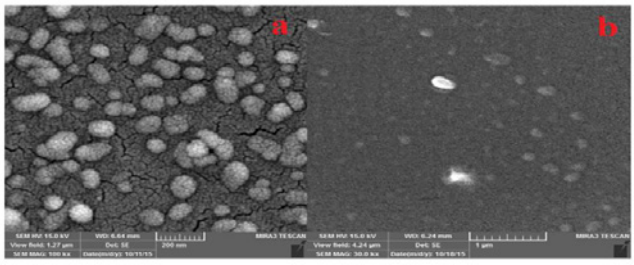

Figure 11: SEM image of Ag-SiO_2-PbTe nano-particles with the magnification of a) 100kx and b) 30kx.

EPS. The size of air bubbles inside the material is different from 200-500μm. These bubbles result in a decrease of refractive index in the polystyrene. With an increase in the size and number of the air bubbles, the refractive index can become near to the refractive index of the air. The refractive index of synthesized EPS is measured about 1.02 by an ellipsometer system (SE800).

The purity and crystallinity of the synthesized Ag-SiO_2-PbTe nanoparticles were examined using powder X-Ray Diffraction (XRD). XRD pattern of nanoparticles is shown in Figure 10. The peaks appeared at 2θ=19.85°, 27.78°, 39.52°, 49.07°, 56.78° are related to (211), (200), (220), (222), (400) crystal planes of the synthesized PbTe respectively and 2θ=38.27°, 44.57°, 64.59° are related to (111), (200), (220) crystal planes of the Ag core respectively.

Figure 11a and 11b show the SEM images of the synthesized Ag-SiO_2-PbTe nanoparticles inside the air bubbles of EPS. The images show that the size of synthesized nanoparticles is about 110nm.

Figure 12 and 13 show absorption and transmission spectrum of the synthesized Ag-SiO_2-PbTe nanoparticles in the host medium of

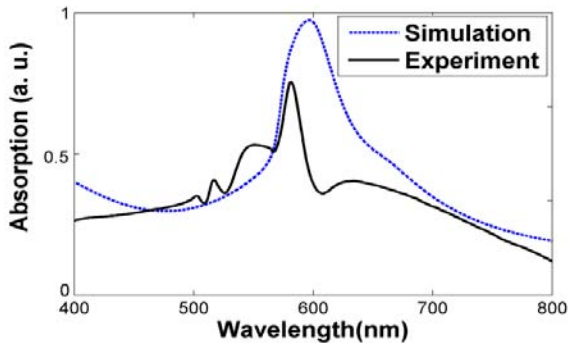

Figure 12: Experimental (black curve) and theoretical (blue curve) absorption spectra of the Ag-SiO_2-PbTe nanoparticles in the host medium of foam.

foam in broadband frequency. Figure 12 shows absorption spectra that demonstrate an intense absorption peak of about 580nm (black curve). The simulation result obtained by equation (10) (blue curve) has a good agreement with the experimental result. Figure 13 shows transmission spectra that demonstrate absorption peak at about 580nm (black curve). The simulation result (blue curve) obtained *via* equation (11) has good agreement with the experimental result too [31].

$$s_{11} = \frac{(-1+e^{2idk_0n})(-1+Z^2)}{-(-1+Z)^2+e^{2idk_0n}(1+Z)^2} \qquad (10)$$

$$s_{21} = \frac{4^{eidk_0n}Z}{-(-1+Z)^2+e2idk_0n(1+Z)^2} \qquad (11)$$

where k_0 is the free space wave-vector, ? is the refraction index, ? is the impedance, and d is the nano-composite thickness (d=125 nm).

In these simulations (For comparing theoretical and simulation results) radius of nanoparticles is considered to be 54nm (Figure 12 and 13) in which the particles have r_1=31 nm, r_2=36nm, and r_3=56nm for core, middle and outer layers respectively with filling factor of 0.38.

Figure 14 shows the effective refractive index of the mentioned structure. Comparing this figure with Figure 6 (negative refractive index of particles with a radius of 62nm) shows that when we go to the shorter wavelengths overlapping between effective permittivity and permeability decreases so the band frequency of the negative refractive index becomes narrow.

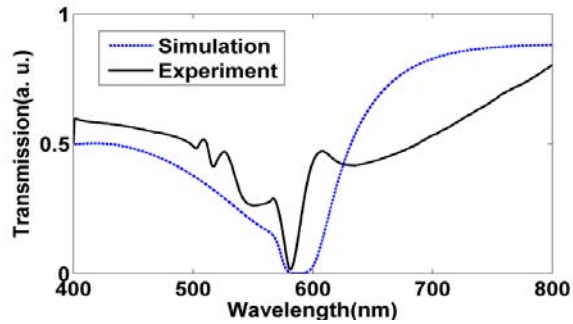

Figure 13: Experimental (black curve) and theoretical (blue curve) absorption transmission spectra of the Ag-SiO_2-PbTe nanoparticles in the host medium of foam.

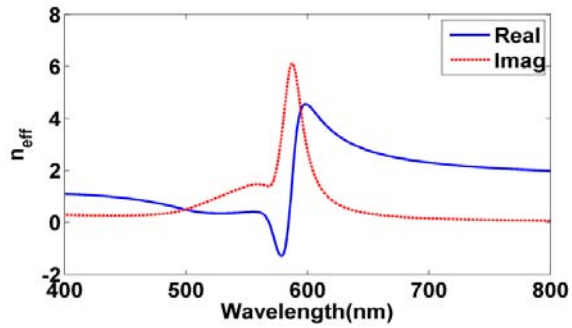

Figure 14: Real and Imaginary parts of the effective refractive index for the Ag-SiO_2-PbTe nano-shells for the random arrangement of nanoparticles in the host medium of foam as a function of wavelength with radius 31nm, 36nm, and 56nm for core middle layer and outer layer respectively.

Summery

In this paper, a metamaterial based on Ag-SiO_2-PbTe nanoparticles dispersed in expanded polystyrene (foam) as a host medium for the realization of a broadband negative refractive index at the visible spectrum is designed and synthesized. The electric and magnetic scattering coefficients of this structure have been calculated using the Mie theory. The inner core (Ag) induced electric responses while the outer layer (PbTe) provides magnetic response and sweeping of the middle layer (SiO_2) can lead to a blue-shift of electric response. Overlapping between electric and magnetic resonance could be realized by designing the radii of the nano-shells. Then the negative electric and magnetic resonances lead to a negative refractive index with a random distribution of nanoparticles in the host medium. The superposition effect and doped semiconductor were respectively applied to broaden the band frequencies with negative permeability and permittivity; so the negative refractive index was broadened about 103nm in the visible band. The broadband negative refractive index using the random distribution of core-shell nanoparticles arises from the proposed metamaterial that has an anisotropic structure. For the realization of the designed structure, Ag-SiO_2-PbTe nanomaterials are synthesized and characterized, and dispersed in expanded polystyrene (Foam). Characterization of synthesized material confirmed the creation of uniform Ag-SiO_2-PbTe nanometal material. The absorption and transmission spectra of nano-composite structures illustrate a good agreement with simulation results at about 580nm.

References

1. T Ergin, N Stenger, P Brenner, JB Pendry, M Wegener. Three-Dimensional Invisibility Cloak at Optical Wavelengths. Science. 2010; 328: 337-339.
2. Y Liu, X Zhang. Recent Advances in Transformation Optics. Nanoscale. 2012; 4: 5277-5292.
3. D Diedrich, A Rottler, D Heitmann, S Mendach. "Metal–Dielectric Metamaterials for Transformation-Optics and Gradient-Index Devices in the Visible Regime". New Journal of Physics. 2012; 14: 053042.
4. D Schurig, JJ Mock, BJ Justice, SA Cummer, JB Pendry, AF Starr, et al. Metamaterial Electromagnetic Cloak at Microwave Frequencies. Science. 2006; 314: 977-980.
5. Y Cui, KH Fung, J Xu, H Ma, Y Jin, S He, et al. Ultra broadband Light Absorption by a Sawtooth Anisotropic Metamaterial Slab. Nano letters. 2012; 12: 1443-1447.

6. O Paul, R Beigang, M Rahm. Highly Selective Terahertz Band pass Filters Based on Trapped Mode Excitation. Optics express. 2009; 17: 18590-18595.

7. JB Pendry. Negative Refraction Makes a Perfect Lens. Physical review letters. 2000; 85: 3966-3969.

8. Y Dong, T Itoh. Metamaterial-Based Antennas. Proceedings of the IEEE. 2012; 100: 2271-2285.

9. H Torres-Silva, DT Cabezas. Chiral Seismic Attenuation with Acoustic Metamaterials. Journal of Electromagnetic Analysis and Applications. 2013; 5: 10-15.

10. DR Smith, WJ Padilla, DC Vier, SC Nemat-Nasser, S Schultz. Composite Medium with Simultaneously Negative Permeability and Permittivity. Physical review letters. 2000; 84: 4184.

11. Jiang, Wei Xiang, Shuo Ge, Tiancheng Han, Shuang Zhang, Muhammad Qasim Mehmood, et al. Shaping 3D Path of Electromagnetic Waves Using Gradient-Refractive-Index Metamaterials. Advanced Science. 2016; 3.

12. Liu Na, Hongcang Guo, Liwei Fu, Stefan Kaiser, Heinz Schweizer and Harald Giessen. Three-dimensional photonic metamaterials at optical frequencies. Nature materials. 2008; 7: 31-37.

13. Shalaev Vladimir M. Optical negative-index metamaterials. Nature photonics. 2007; 1: 41-48.

14. Dolling Gunnar, Christian Enkrich, Martin Wegener, Costas M Soukoulis and Stefan Linden. Low-loss negative-index metamaterial at telecommunication wavelengths. Optics letters. 2006; 31: 1800-1802.

15. Chettiar Uday K, Alexander V Kildishev, Hsiao-Kuan Yuan, Wenshan Cai, Shumin Xiao, et al. Dual-band negative index metamaterial: double negative at 813nm and single negative at 772nm. Optics Letters. 2007; 32: 1671-1673.

16. Lezec Henri J, Jennifer A Dionne, and Harry A Atwater. Negative refraction at visible frequencies. Science. 2007; 316: 430-432.

17. Burgos Stanley P, Rene de Waele, Albert Polman and Harry A Atwater. A single-layer wide-angle negative-index metamaterial at visible frequencies. Nature Materials. 2010; 9: 407-412.

18. Atre Ashwin C, Aitzol García-Etxarri, Hadiseh Alaeian and Jennifer A Dionne. A broadband negative-index metamaterial at optical frequencies. Advanced Optical Materials. 2013; 1: 327-333.

19. WL Barnes, A Dereux, TW Ebbesen. "Surface Plasmon Subwavelength Optics". Nature. 2003; 424: 824-830.

20. DÖ Güney, T Koschny, CM Soukoulis. Surface Plasmon Driven Electric and Magnetic Resonators for Metamaterials. Physical Review B. 2011; 83: 045107.

21. Seo Byoung-Joon, Tetsuya Ueda, Tatsuo Itoh, and Harold Fetterman. "Isotropic left-handed material at the optical frequency with dielectric spheres embedded in negative permittivity medium". Applied physics letters. 2006; 88: 161122.

22. K Kodali, MV Schulmerich, R Palekar, X Llora, R Bhargava. Optimized Nanospherical Layered Alternating Metal-Dielectric Probes for Optical Sensing. Optics express. 2010; 18: 23302-23313.

23. D Wu, S Jiang, Y Cheng, X Liu. Three-Layered Metallodielectric Nanoshells: Plausible Meta-Atoms for Metamaterials with Isotropic Negative Refractive Index at Visible Wavelengths. Optics express. 2013; 21: 1076-1086.

24. Paniagua-Domínguez R, F López-Tejeira, R Marqués and José Antonio Sánchez-Gil. Metallo-dielectric core-shell nanospheres as building blocks for optical 3D isotropic negative-index metamaterials. arXiv preprint arXiv. 2011; 13: 123017.

25. NH Shen, T Koschny, M Kafesaki, CM Soukoulis. Optical Metamaterials with Different Metals. Physical Review B. 2012; 85: 075120.

26. CF Bohren, DR Huffman. Absorption and scattering of light by small particles. John Wiley & Sons. 1998.

27. D Wu, X Xu, X Liu. Tunable Near-Infrared Optical Properties of Three-Layered Metal Nanoshells. The Journal of chemical physics. 2008; 129: 074711.

28. M Keshavarz, S Khosravi, A Rostami, G Rostami, M Dolatyari. Broadband Negative Refractive Index in the Visible Spectrum. In Proceedings of the 3rd International Conference on Photonic, Berlin, Germany. 2015: 113-117.

29. MS Wheeler, JS Aitchison, M Mojahedi. Coated Nonmagnetic Spheres with a Negative Index of Refraction at Infrared Frequencies. Physical Review B. 2006; 73: 045105.

30. J Shen, X Cao, L James Lee. Synthesis and Foaming of Water Expandable Polystyrene-Clay Nanocomposites. Polymer. 2006; 47: 6303-6310.

31. CG Parazzoli, RB Greegor, K Li, BEC Koltenbah, M Tanielian. "Experimental Verification and Simulation of Negative Index of Refraction Using Snell's Law". Physical Review Letters. 2003; 90: 107401.